Annals of Nuclear Energy 177 (2022) 109305

Contents lists available at ScienceDirect

Annals of Nuclear Energy

journal homepage: www.elsevier.com/locate/anucene

Study on the operating conditions of centrifuges and their individual separative power in a stage of an isotope separation cascade

Renata R.R. de Paula [a,*], Sylvana C.P. Migliavacca [b], Roberto Guardani [a]

[a] University of Sao Paulo, Chemical Engineering Department, Av Luciano Gualberto 380 Tv 3, Sao Paulo 05508-000, Brazil
[b] IPEN - Nuclear and Energetic Research Institute, Av. Prof. Lineu Prestes 2242, Sao Paulo 05508-000, Brazil

ARTICLE INFO

Article history:
Received 19 January 2022
Received in revised form 23 May 2022
Accepted 21 June 2022
Available online 1 July 2022

2020 MSC:
08-08

Keywords:
Cascade
Separative power
Gas centrifuge
Mathematical model
Uranium enrichment

ABSTRACT

Since the ideal cascade theory, several mathematical models have been developed to improve the understanding of isotopic separation cascades. Despite numerous advances in modeling multicomponent and transient cascades, there has not yet been a model that takes into account the individual centrifuges' operating conditions and separative power.

This study analyses how the number of centrifuges in a stage relates to the pressure drop in the pipes, which in turn affects the centrifuges' separative power. It estimates the local operating conditions, checks them against the mass balances in the pipes and, then, calculates the separative performance of the centrifuges.

Results were presented for a stage with 40 generic centrifuges. There was a sharp pressure drop in the extremities of the stage that caused roughly 15% and 30% pressure loss in the feed and product pipes, respectively, which caused the last centrifuge to yield a separative power 14% lower than the first one.

1. Introduction

The theory and mathematical modeling of isotope separation cascades for a binary mixture of isotopes was first described by Karl Cohen in the 50s. Cohen (1951) made several simplifying assumptions in order to develop a theory as general as possible to permit extension to a set of different separation systems. It is known as the theory of the ideal cascade and it is the main reference for cascade up to the present date.

Two of the main assumptions are that (1) the separation factors of the stages are known and constant for all the stages; and (2) the merging streams have equal concentrations of each isotope (which is called the non-mixing condition). Thus the ideal cascade theory overlooks the separation factor of each separative unit and the influence it exerts on the stages.

This theory has, since, been studied and improved by other authors throughout the second half of the 20th century. Laguntsov (1973) added to the model the possibility of arbitrary separation factors for each stage and Palkin (1997) added to it the mixture of non-identical concentration streams. These developments brought to the mathematical model a greater proximity to the non-ideal cascade's operating conditions.

Then, based on the developments above, Portoghese (2002) created a semi-empirical model by adding empirical correlations for the separative units. The main assumption was that the separative units in each stage are subject to identical flow conditions, so an empirical model for one centrifuge could be applied to an entire stage. Thus the separation factor was no longer arbitrarily chosen since it became a direct result of calculations for the average flow conditions in each stage.

Several authors have improved other aspects of cascade modeling since then, such as multicomponent mixture of isotopes (de la Garza et al., 1961; Kucherov and Minenko, 1965; Sulaberidze and Borisevich, 2001; Palkin et al., 2002; von Halle, 1987; Song et al., 2010) and transient process (Orlov et al., 2016; Orlov et al., 2018; Cao et al., 2004). However these developments have not yet mapped the flow conditions for each individual centrifuge and the stage performance as a result thereof.

This study proposes a mathematical model capable of taking into account the pipe flow conditions at each individual centrifuge, and thus represent a more rigorous and realistic approach to the description of isotope separation cascades.

* Corresponding author.
E-mail address: renatarrpaula@usp.br (R.R.R. de Paula).

https://doi.org/10.1016/j.anucene.2022.109305
0306-4549/

Nomenclature

a	Centrifuge radius	M	Molecular mass
A_{D_P}	Cross section area of diameter D_P	μ	Viscosity of the gas
A_{D_W}	Cross section area of diameter D_W	N	Number of centrifuges in a stage
γ	Isentropic expansion factor	P	Stage product flow rate
D	Coefficient of self-diffusion	pf	Feed pressure
D_I	Pipe internal diameter	pp	Product pressure
D_P	Product orifice plate diameter	pw	Waste pressure
D_W	Waste orifice plate diameter	R	Universal gas constant
δU	Separative power	r_1, r_2	Two-shell radii (Glaser, 2008)
F	Stage feed flow rate	r_c	Critical ratio for choked flow of the UF_6 gas
f	Fanning friction factor	ρ	Density of the gas
G	Individual feed flow rate	T	Gas temperature
i	Subscript for the centrifuges in a stage	Θ	Cut
j	Subscript for the stages in a cascade	v_a	Peripheral velocity of the centrifuge rotor
k	Proportionality constant between G_i and pf_i	W	Stage waste flow rate
L	Internal countercurrent flow	Z	Centrifuge rotor length
l	Pipe length between centrifuges	Z_p	Rectifier length

2. Generic Centrifuge Model

Due to the confidential nature of isotope separation ultracentrifuges, a generic centrifuge model was created to present the results of the proposed mathematical model. It was obtained by combining the analytical model for the separative power of Ratz (1983), the geometric characteristics and operating parameters of the Rome centrifuge used by Glaser (2008), and the empirical model for the pressure at the waste stream developed by An et al. (2019).

Additionally, the feed flow G and the feed pressure pf of this generic centrifuge are assumed to be directly proportional due to choked flow conditions that are created via the insertion of an orifice plate in the feed pipe.

2.1. Separative Power and Rome Centrifuge

In his study, Glaser (2008) presented a comprehensive explanation of the analytical model of Ratz (1983) and its application for the Rome centrifuge parameters. Eqs. (1)–(5) show the calculation of the separative power as a function of the flow conditions that vary throughout the stage.

$$\delta U(G,\Theta,pp) = \delta U_{ratz} = \frac{1}{2}G\Theta(1-\Theta)\left(\frac{\Delta M}{2RT}v_a^2\right)^2\left(\frac{r_2}{a}\right)^4 \left(1-\left(\frac{r_1}{r_2}\right)^2\right)^2\left(\left(\frac{1+L/G}{\Theta}\right)(1-exp(-A_pZ_p))^2 + \frac{L/G}{1-\Theta}(1-exp(-A_w(Z-Z_p)))\right) \quad (1)$$

with

$$A_p = \frac{2\pi D\rho}{\ln r_2/r_1}\frac{\Theta}{G(1+L/G)(1-\Theta+L/G)}, \quad (2)$$

$$A_w = \frac{2\pi D\rho}{\ln r_2/r_1}\frac{(1-\Theta)}{G(L/G)(1-\Theta+L/G)}, \quad (3)$$

$$Z_p = \frac{1}{2}Z, \quad (4)$$

$$D\rho = 2.2\,10^{-5}\frac{kg}{ms}, \quad (5)$$

where G is the feed rate of the centrifuge, Θ is the cut, $\Delta M = 0.003\,kg/mol$ is the molar weight difference for a binary mixture of ^{235}U and ^{238}U, R is the universal gas constant, T is the average temperature of the gas, D is the coefficient of self-diffusion, ρ is the density of the gas, r_1 and r_2 are the two-shell radii, a is the centrifuge radius, v_a is the peripheral velocity of the rotor, Z is the centrifuge length, Z_p is the rectifier length and L is the internal countercurrent flow, all in SI units.

Table 1 shows the parameters of the Rome centrifuge according to Glaser (2008) and the value of r_2/a estimated for this generic model.

The internal countercurrent flow L was presented by Glaser (2008) along with the characteristic parameter countercurrent-to-feed ratio L/G, which was assumed constant and claimed to typically assume values between 2 and 4. In this study, however, for simplicity and feasibility of the mathematical modeling and simulation, the countercurrent flow L is assumed to be directly proportional to the product pressure pp. This relationship is intuitive, given that the smaller the valve aperture is, the greater pp and the countercurrent flow are, *i.e.*, greater values of pp correspond to greater values of the countercurrent flow. However it has not yet been proved or derived theoretically in literature and must, therefore, be treated as an additional assumption for the generic centrifuge model.

Thus, the countercurrent-to-feed ratio is represented by $L/G = 2\,pp/G$ with pp in Pa and G in kg/year. The proportionality constant 2 was estimated according to the assumption of Glaser (2008) that L/G typically takes values between 2 and 4.

2.2. Waste Pressure

An et al. (2019) developed an empirical model for the waste pressure pw as a function of pp, G, and Θ (Eqs. (6)–(8)), which was adopted in this study as part of the generic centrifuge model.

Table 1
Rome centrifuge parameters as applied by Glaser (2008).

Parameter	Value
v_a (m/s)	600
Z (cm)	200
a (cm)	10
r_1/r_2	0.843
r_2/a	0.9

$$pw = pw(pp, \Theta, G) = \frac{pp - \delta}{k\prime} \tag{6}$$

$$k\prime = a_1 + b_1 \Theta G \tag{7}$$

$$\delta = a_2 + b_2 \Theta G + c_2 G \tag{8}$$

where pp and pw are in Torr, G is in mg/s, $a_1 = 0.62367, b_1 = -0.0085\, s/mg, a_2 = -0.02339, b_2 = -0.008876\ s/mg$, and $c_2 = 0.00219\, s/mg$.

2.3. Proportionality between pf and G

Given the choked flow assumption in the feed pipe, there is a direct proportionality between pf and G (Fay, 1994; Kayser and Shambaugh, 1991), as in Eq. 9.

$$G = k\, pf \tag{9}$$

For choked conditions caused by the insertion of an orifice plate, usually the proportionality constant is determined empirically. For this generic centrifuge model, two nominal operating conditions were arbitrarily adopted in the simulations: (1) G_{nom} = 500 kg/year, $pf_{nom} = pp_{nom}$ = 1000 Pa, k = 0.5; and (2) G_{nom} = 2500 kg/year, $pf_{nom} = pp_{nom}$ = 1000 Pa, k = 2.5.

3. Stage Model

For a generic stage j in a cascade, the feed flow rate comes both from the waste W_{j+1} of stage $(j+1)$ and the product P_{j-1} of stage $(j-1)$.

For the purpose of this study, consider a cascade made only by one stage as in Fig. 1. The flow rates from both ends are assumed to be equal to half of the stage total feed, *i.e.*, $F_1 = F_{N+1} = F_{total}/2$.

F_{total} is given by Eq. 10, where G_{nom} is the nominal feed flow rate for the generic centrifuge and N is the number of centrifuges in the stage.

$$F_{total} = N\, G_{nom} \tag{10}$$

F varies throughout the pipe as the centrifuges are fed with flow rate G_i, where i represents the number of the centrifuge in the stage. For this reason, F has a subscript representing its position, F_i. Similarly, the product and waste flow rates are given by P_i and W_i and the pressure in the pipes by pf_i, pp_i and pw_i, respectively.

Assuming the following conditions: (1) constant pipe internal diameter D_I, (2) constant temperature T, (3) constant pipe length l between centrifuges, (4) steady state, and (5) viscous fluid flow, it is possible to mathematically model the flow conditions throughout the pipe.

In this study, two different approaches were adopted: (1) constant $G = G_{nom}$ and (2) $G_i = k\, pf_i$ in choked flow conditions. The first one is simpler and can be solved analytically, allowing the visualization of the relationship between variables and pressure loss. The second one is more complex and realiable, but requires iterative calculations.

3.1. Constant $G_i = G_{nom}$

Considering that all centrifuges have constant individual feed flow rate G_{nom}, F_i follows an arithmetic progression until the center of the pipe with common difference equal to $-G_{nom}$, as in Eq. 11.

$$\frac{F_{total}}{2} \rightarrow \left(\frac{F_{total}}{2} - G_{nom}\right) \rightarrow \left(\frac{F_{total}}{2} - 2G_{nom}\right) \rightarrow \ldots \rightarrow 0 \tag{11}$$

At $i = N/2$, the flow rate $F_{N/2}$ is approximately zero, and then it grows back in the opposite direction of the flow with common difference G_{nom}.

The pressure difference between two adjacent centrifuges in the feed pipe is given by Poiseuille law, as in Eq. 12, for an ideal gas, constant temperature, laminar and incompressible flow:

$$pf_i - pf_{i+1} = \frac{128\, F_i\, l\, \mu\, R\, T}{M\, pf_{aver}\, \pi\, D_I^4} \tag{12}$$

where D_I is the pipe internal diameter, l is the length of the pipe between two adjacent centrifuges, M is the molecular mass of the gas, μ is the viscosity of the gas and pf_{aver} is the average pressure between the two points. All in SI units.

Since pf_{aver} is approximately the average pressure of the entire feed pipe, it is considered constant and equal to the nominal feed pressure for the generic centrifuge pf_{nom}.

The largest pressure difference in the feed pipe occurs between any of the extremeties (pf_1 or pf_N) and the central point $pf_{N/2}$, where the flow rate is nearly zero. It can be estimated by applying Poiseuille's law and the sum of the $N/2$ first terms of the arithmetic progression as follows.

$$pf_1 - pf_{N/2} = (pf_1 - pf_2) + (pf_2 - pf_3) + \ldots + (pf_{N/2-1} - pf_{N/2}) \tag{13}$$

$$pf_1 - pf_{N/2} = \frac{128\, l\, \mu\, R\, T}{M\, pf_{nom}\, \pi\, D_I^4}\left[\left(\frac{F_{total}}{2}\right) + \left(\frac{F_{total}}{2} - G_{nom}\right) + \ldots + 0\right] \tag{14}$$

$$pf_1 - pf_{N/2} = \frac{128\, l\, \mu\, R\, T}{M\, pf_{nom}\, \pi\, D_I^4}\frac{(F_{total}/2 + 0)}{2} N/2 \tag{15}$$

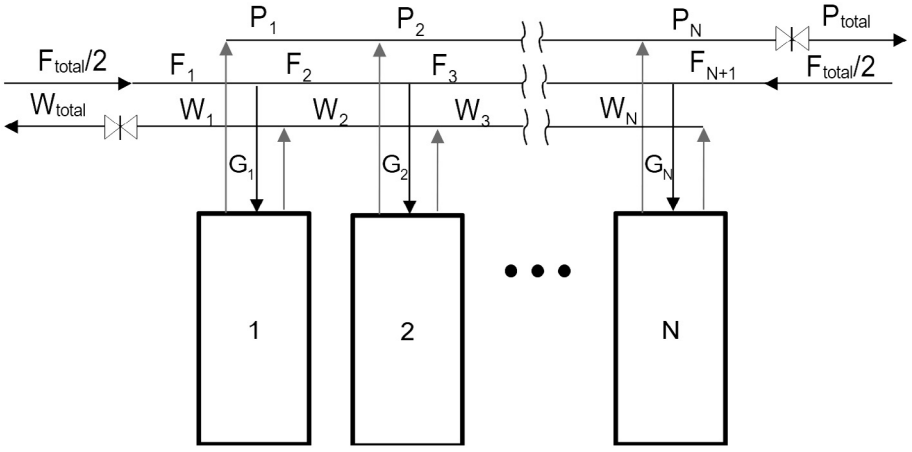

Fig. 1. One-stage cascade piping layout.

Applying Eq. 10, the maximum pressure loss in the feed pipe is given by Eq. 16.

$$pf_1 - pf_{N/2} = \frac{128\, l\, \mu\, R\, T}{M\, pf_{nom}\, \pi\, D_l^4} \frac{G_{nom}}{8} N^2 \tag{16}$$

An analogous analysis for the product and waste pipes is given by Eq. 17 and 18.

$$pp_1 - pp_N = \frac{128\, l\, \mu\, R\, T}{M\, pp_{nom}\, \pi\, D_l^4} \frac{\Theta_{nom}\, G_{nom}}{4} N^2 \tag{17}$$

$$pw_N - pw_1 = \frac{128\, l\, \mu\, R\, T}{M\, pw_{nom}\, \pi\, D_l^4} \frac{(1-\Theta_{nom})\, G_{nom}}{4} N^2 \tag{18}$$

Therefore, for laminar and incompressible flow with constant centrifuge feed equal to G_{nom}, the overall pressure loss in the pipe is proportional to N^2.

3.2. Choked flow $G_i = k\, pf_i$

By assuming that a physical restriction is placed before every centrifuge in a way that the individual feed flow G_i becomes chocked and, therefore, directly proportional to the upstream pressure pf_i, then the local feed flow rate between two adjacent centrifuges, $F_i - F_{i+1}$, will no longer behave as an aritmetic progression and G_i will be a function of pf_i due to the chocked flow condition.

For this reason, to estimate F_i, G_i and pf_i for every i in the feed pipe it is necessary to apply an iterative calculation procedure.

Since such algorithm estimates the flow conditions at each point of the pipe, the flow is not assumed to be laminar anymore, so the pressure loss in the pipe between two adjacent centrifuges is calculated by Bernoulli's equation.

The calculation of operating conditions throughout the stage can be divided in two sequencial steps: (1) feed flow conditions and (2) product and waste flow conditions.

3.2.1. Feed Flow Conditions

The calculation begins at the left end of the pipe by assigning the flow rate value to the variable $F_1 = F_{total}/2$, where the centrifuge $i = 1$ is placed. The local pressure pf_1 is estimated to be the nominal value of the centrifuge pf_{nom} and the feed flow G_1 is, then, calculated through Eq. 9.

Once G_1 is known, F_2 is calculated by Eq. 19. Then, before applying Bernoulli's equation to estimate the pressure loss, it is necessary to know the flow regime by calculating the Reynolds number.

$$F_2 = F_1 - G_1 \tag{19}$$

For $2100 < Re < 5000$, where the flow is transitional and the Fanning friction factor is not well defined in literature (Bird et al., 2002), the same factor for turbulent flow in a hydraulically smooth piping is used.

Then pf_2 is calculated by Eq. 20 and G_2 by Eq. 9.

$$pf_2 = pf_1 - \frac{\rho\, l 2 f}{D_l} \left(\frac{4F_2}{\rho \pi D_l^2}\right)^2 \tag{20}$$

where f is the Fanning friction factor.

This procedure is followed until the middle of the pipe, where F_i is less than G_i. Then G_i starts to be added instead of subtrated from the pipe flow.

The flow F_{N+1} obtained at the right end of the pipe must, then, be equal to $F_{total}/2$ to satisfy the mass balance of the stage. While $|F_{N+1} - F_{total}/2|$ is greater than a pre-defined tolerance, the procedure restarts iteratively with a new estimation of pf_1 at each iteration.

3.2.2. Product and Waste Flow Conditions

Considering the layout of the product and waste pipes of Fig. 1, the control valves apertures are set so that the stage cut equals the centrifuge nominal cut, *i.e.*, $\Theta_{stage} = \Theta_{nominal}$. Thus the expected product and waste flow rates, P^*_{total} and W^*_{total} respectively, can be obtained using the cut definition, Eq. 21, and the total mass balance, Eq. 22.

$$P^*_{total} = \Theta_{stage}\, F_{total} \tag{21}$$

$$W^*_{total} = F_{total} - P^*_{total} \tag{22}$$

It is assumed that the flow through the control valves is chocked. This is a reasonable assumption because, due to the existence of compressors after the valves, the ratio between downstream and upstream pressure is lower than the critical ratio for chocked flow. For this reason, the flow rates are directly proporcional to the upstream pressures and function of the valve geometry and UF_6 properties.

Aiming to generalize this study case, the control valves of Fig. 1 were treated as equivalent orifice plates of diameters D_P and D_W. Thus the flow rates $P_N = P^*_{total}$ and $W_1 = W^*_{total}$ are related to the upstream pressure for a critical orifice (Kayser and Shambaugh, 1991) by Eqs. 23 and 24, respectively.

$$P_N = \frac{A_{D_P}\, M\, pp_N}{R\, T}\, r_c^{1/\gamma} \sqrt{\frac{2\gamma\, R\, T}{M\,(\gamma-1)}\,(1 - r_c^{(\gamma-1)/\gamma})} \tag{23}$$

$$W_1 = \frac{A_{D_W}\, M\, pw_1}{R\, T}\, r_c^{1/\gamma} \sqrt{\frac{2\gamma\, R\, T}{M\,(\gamma-1)}\,(1 - r_c^{(\gamma-1)/\gamma})} \tag{24}$$

where r_c is the critical ratio for the UF_6 gas, γ is the isentropic expansion factor of the UF_6, and A_{D_P} and A_{D_W} are the cross section areas, in m^2, of the equivalent orifices.

Because the valves apertures can assume any positive value, the diameters D_P and D_W are chosen to be the values that provide $\Theta_{stage} = \Theta_{nom}$. Therefore, through algebraic manipulations of Eqs. 23 and 24, it is possible to obtain the expected upstream pressures pp^*_N and pw^*_1.

For convenience, the calculation procedure begins at the right end of the pipes by assuming $pp_N = pp^*_N$ and estimating the cut Θ_N of the last centrifuge. Since the values of pp_N and G_N are already known, it is possible to apply Eqs. 1 and 6 to determine, respectively, the separative power δU_N and pw_N of the Nth centrifuge.

Then, applying Eqs. 25 and 26, the flow rates P_{N-1} and W_{N-1} are estimated.

$$P_{N-1} = P_N - \Theta_N\, G_N \tag{25}$$

$$W_{N-1} = W_N + (1 - \Theta_N)\, G_N \tag{26}$$

Then, Bernoulli's equation is applied observing the flow regime given by the Reynolds number and the direction of the pressure gradient in each pipe, as in Eqs. 27 and 28.

$$pp_{N-1} = pp_N + \frac{\rho\, l 2 f}{D_l} \left(\frac{4P_{N-1}}{\rho \pi D_l^2}\right)^2 \tag{27}$$

$$pw_{N-1} = pw_N - \frac{\rho\, l 2 f}{D_l} \left(\frac{4W_{N-1}}{\rho \pi D_l^2}\right)^2 \tag{28}$$

Once pp_{N-1}, pw_{N-1} and G_{N-1} are known, it is possible to calculate Θ_{N-1} through Eq. 6. The same procedure is followed for each centrifuge until the left end of the pipes.

At $i = 1$, the pressure pw_1 calculated is, then, compared to the expected pressure pw^*_1. While $|pw_1 - pw^*_1|$ is greater than a

Table 2
Simulated operating conditions.

Scenario	k	G_{nom}	$pf_{nom} = pp_{nom}$	pw_{nom}	l	D_l	T	Θ_{nom}
(1)	0.5	500 kg/year	1000 Pa	1800 Pa	0.5 m	1 in	25°C	0.5
(2)	2.5	2500 kg/year	1000 Pa	3600 Pa	0.5 m	1 in	25°C	0.5

pre-defined tolerance, the procedure restarts iteratively with a new estimation of Θ_N at each iteration.

4. Results and Discussion

Two simulation scenarios were adopted to analyze how the number of centrifuges in a stage affects the pressure loss in the pipes: (1) entirely laminar flow, and (2) mixture of flow regimes. The nominal operating conditions are shown in Table 2.

The simulations compare the overall pressure loss in the feed pipe, Δpf, for the constant $G_i = G_{nom}$ model and the choked flow $G_i = k\, pf_i$ model. Figs. 2 and 3 show the results relative to the nominal pressure in the feed pipe, pf_{nom}, for scenarios 1 and 2, respectively.

For entirely laminar flow, as in Fig. 2, the pressure loss is a function of the squared number of centrifuges, N^2, as predicted by the $G_i = G_{nom}$ model. Even when the individual feed is proportional to the feed pressure, $G_i = k\, pf_i$, the profile is still parabola-shaped. This means that, when designing a cascade, the number of centrifuges in each stage should be carefully analyzed to minimize pressure drop. The farther the operating pressures are from the nominal conditions, the lower the stage overall separative power will be.

For a mixture of flow regimes, as in Fig. 3, the models present very different profiles. This is expected, since the complete laminar flow assumption for the $G_i = G_{nom}$ model is not valid in scenario 2. Fig. 4 shows in-depth pressure drop in this scenario for the stage with 40 centrifuges. The local Reynolds number and the feed pressure profile were calculated by the $G_i = k\, pf_i$ model.

It is noticeable that, for the non-laminar flow at the extremities ($Re > 2100$), the pressure drop between adjacent centrifuges is greater than at the mid-section. It is also noticeable that the minimum pressure occurs exactly at the middle of the stage ($N_i = 20$), where there is a change in the direction of the feed pipe flux. This occurs due to the initial hypothesis that the flow rates in both extremities of the feed pipe are exactly half of the total flow ($F_{total}/2$). If, however, they where different from each other, the minimum point would be localized somewhere else.

When analyzing the profiles of the local pressures for all the pipes (feed, product and waste), Fig. 5 shows that centrifuges at

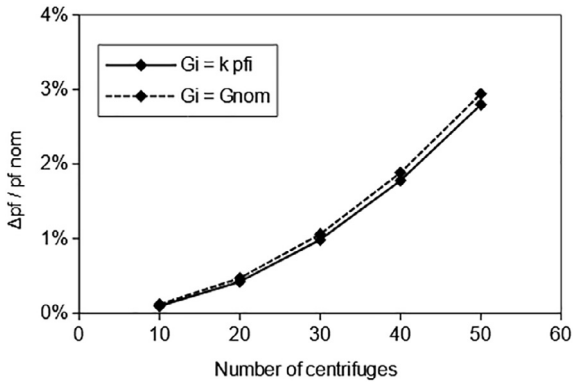

Fig. 2. Relative pressure loss as a function of the number of centrifuges in the stage for a entirely laminar flow in scenario 1.

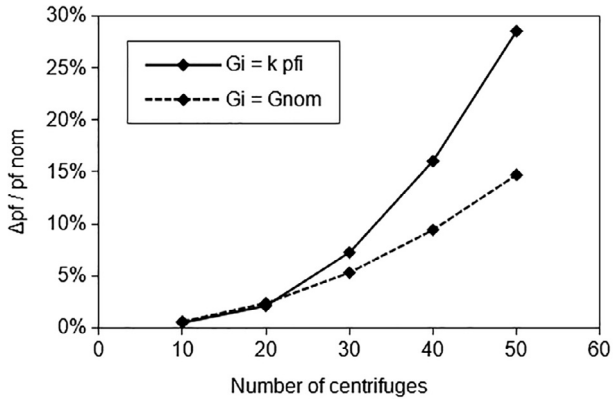

Fig. 3. Relative pressure loss as a function of the number of centrifuges in the stage for a mixture of flow regimes in scenario 2.

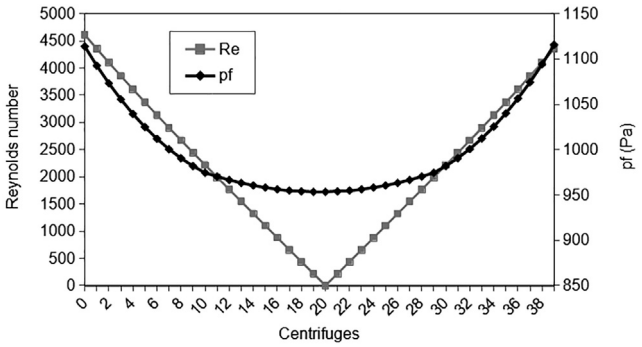

Fig. 4. Feed pipe local pressure and Reynolds number for a stage with 40 centrifuges in scenario 2.

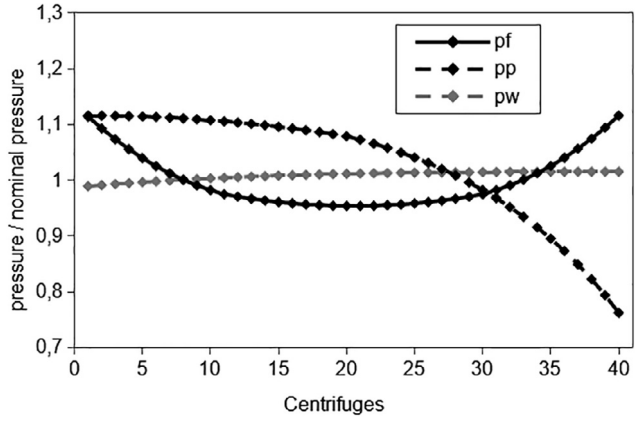

Fig. 5. Pressure ratio profiles of the feed, product and waste pipes for a stage with 40 centrifuges in scenario 2.

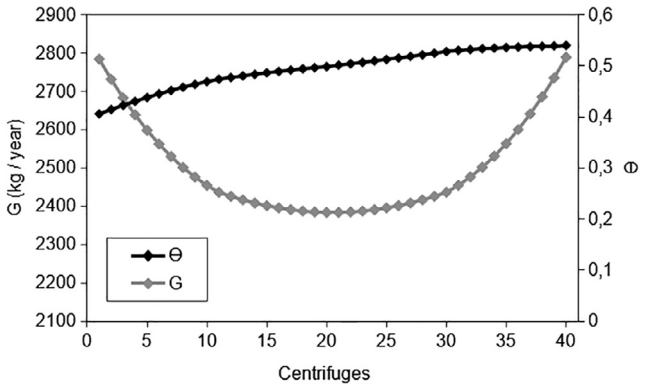

Fig. 6. Individual feed flow rate and cut profiles for a stage with 40 centrifuges in scenario 2.

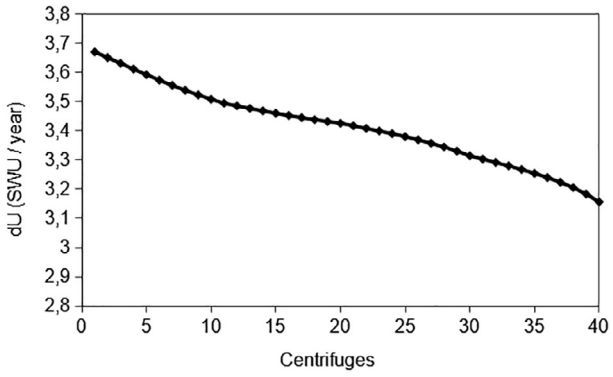

Fig. 7. Separative power profile for a stage with 40 centrifuges in scenario 2.

different extremities are subject to significantly different conditions. The pressure drops roughly 15% and 30% in the feed and product pipes, respectively. The waste pressure ratio profile is approximately constant due to the higher nominal pressure.

This local difference in operating pressure causes the individual cut and feed flow rate of centrifuges to diverge significantly, which yields different individual separative power as well, as seen in Figs. 6 and 7, respectively. The first centrifuge, at the right extremity, has a separative power 14% higher than the last one, at the left extremity. It is worth noting, though, that different gas centrifuges designs might amplify or minimize the observed behavior.

5. Conclusions

Unlike in previous cascade mathematical models, whose operating conditions are considered uniform throughout each stage, the proposed model calculates the local operating conditions and separative performance of each centrifuge that composes a stage.

Through the $G_i = G_{nom}$ model, it was possible to observe the proportionality of the pressure loss in the pipes, Δpf, with the squared number of centrifuges N^2 in the stage for an entirely laminar flow.

The $G_i = k\,pf_i$ model for choked flow conditions was, then, applied for other flow regimes. The estimated pressure loss dependency on the number of centrifuges when there is transitional or turbulent flow was shown to be of higher order than N^2.

The analysis of two different scenarios, (1) entirely laminar flow and (2) mixture of flow regimes, indicates that, depending on the size of the stage (i.e., number of centrifuges in the stage) the flow regime and the centrifuge model, the centrifuges can be subject to local pressure conditions that are significantly different from the nominal ones. This makes their separative power diverge from one another, which, in turn, may contribute to lower the overall stage separative power.

The results for a generic centrifuge model in a stage with 40 centrifuges showed that the total pressure loss in the feed pipe was aprox. 2% and 15% in scenarios 1 and 2, respectively.

In scenario 2, the extremities of the stage presented a sharp pressure drop due to the transitional flow, with roughly 15% and 30% pressure losses for the feed and product pipes, respectively. The divergence in the operating conditions caused the last centrifuge in the stage to yield a 14% lower separative power from the first one.

These results reveal the importance of knowing the individual operating conditions of the centrifuges in a stage. By applying the proposed approach to the mathematical modeling of stages in a cascade, it could allow a comprehensive understanding of the separation system and a more accurate prediction of its performance. Thus, it represents a significant step towards improving the mathematical modeling and analysis of entire gas centrifuge cascades.

CRediT authorship contribution statement

Renata R. R. de Paula: Conceptualization, Methodology, Software, Formal analysis, Validation, Visualization, Writing - original draft. **Sylvana C.P. Migliavacca:** Resources, Investigation, Validation, Writing - review & editing. **Roberto Guardani:** Supervision, Writing - review & editing.

Declaration of Competing Interest

The authors declare that they have no known competing financial interests or personal relationships that could have appeared to influence the work reported in this paper.

References

An, M., Zhang, Y.N., Zeng, S., Lei, Z., Borisevich, V.D., Smirnov, A.Y., 2019. Numerical study of the hydraulic characteristics of the bi-directionally connected gas centrifuge. In: 15th International Workshop on Separation Phenomena in Liquids and Gases.

Bird, R.B., Stewart, W.E., Lightfoot, E.N., 2002. Transport Phenomena. John Wiley & Sons Inc.

Cao, Y., Zeng, S., Zengguang, L., Ying, C., 2004. Study of a nonstacionary separation method with gas centrifuge cascade. Sep. Sci. Technol. 39 (14), 3405–3429.

Cohen, K., 1951. The Theory of Isotope Separation as Applied to Large Scale Production of 235U. McGraw Hill.

de la Garza, A., Garret, G.A., Murphy, J.E., 1961. Multicomponent isotope separation in cascades. Chem. Eng. Sci., 188–209

Fay, J.A., 1994. Introduction to Fluid Mechanics. MIT Press.

Glaser, A., 2008. Characteristics of the gas centrifuge for uranium enrichment and their relevance for nuclear weapon proliferation. Science and Global Security 16, 1–25.

Kayser, J.C., Shambaugh, R.L., 1991. Discharge coefficients for compressible flow through small-diameter orifices and convergent nozzles. Chem. Eng. Sci. 46 (7), 1697–1711.

Kucherov, R., Minenko, V., 1965. Theory of cascades for separating multicomponent isotope mixtures. At Energy 19, 1290–1300.

Laguntsov, N.I., 1973. Calculation of ideal cascades with arbitrary enrichment per stage. Atomnaya Énergiya 35 (3), 205–207.

Orlov, A., Ushakov, A., Sovach, V., 2016. Mathematical modeling of nonstacionary separation processes in gas centrifuge cascade for separation of multicomponent isotope mixtures. In: MATEC Web of Conferences 72.

Orlov, A.A., Ushakov, A.A., Sovach, V.P., 2018. Mathematical modeling of nonstacionary separation processes in gas centrifuge cascade for separation of tungsten isotopes. J. Eng. Phys. Thermophys. 91 (3).

Palkin, V., Sbitnev, N., Frolov, E., 2002. Calculation of the optimal parameters of a cascade for separating a multicomponent mixture of isotopes. At. Energ. 92 (2), 141–146.

Palkin, V.A., 1997. Optimization of a cascade with arbitrarily specified separation coefficients of the stages. At. Energ. 82 (4).

Portoghese, C.C., 2002. Modelagem matemática do comportamento estático e dinâmico dos parâmetros operacionais de cascatas de separação isotópica por ultracentrifugação. Ph.D. thesis, Instituto de Pesquisas Energéticas e Nucleares.

Ratz, E., 1983. An analytical solution for the separative power of gas centrifuges. In: 5th Workshop on Gases in Strong Rotation.
Song, T., Zeng, S., Sulaberidze, G., Borisevich, V., Xie, Q., 2010. Comparative study of the model and optimum cascades for multicomponent isotope separation. Sep. Sci. Technol. 45 (14), 2113–2118.
Sulaberidze, G., Borisevich, V., 2001. Cascades for separation of multicomponent isotope mixtures. Sep. Sci. Technol. 36 (8–9), 1769–1817.
von Halle, E., 1987. Multicomponent isotope separation in matched abundance ratio cascades composed of stages with large separation factors. In: Proc. 1st Workshop on Separation Phenomena in Liquids and Gases, p. 325.